Fabrication of Ultrathin Silicon Nanoporous Membranes and Their Application in Filtering Industrially Important Biomolecules

Balachandra H. V. Achar, Sudeshna Sengupta, and Enakshi Bhattacharya, *Member, IEEE*

***Abstract*—Ultrathin silicon nanoporous membranes with multiple pores were fabricated using batch processes involving chemical vapor deposition and rapid thermal annealing. Transmission electron microscope images showed the existence of nanopores with an average pore size of 13 nm. Measurement of ionic conduction of electrolytes with varying conductivity across the membranes confirmed the existence of pores and the repeatability of the process. The functional diameter of the pores was determined by analyzing the permeability of several industrially and medically important globular biomolecules of varying sizes such as α-amylase, bovine serum albumin, catalase and xanthine oxidase. Biomolecules with hydrodynamic diameters up to 8 nm passed through the nanopores, whereas the passage of the larger molecules was hindered. The surface charges on the molecules determine the functional diameter of the pores, and hence the permeability, as substantiated by varying the pH of the buffer solution. The filtered proteins were found to be uncleaved from sodium dodecyl sulfate polyacrylamide gel electrophoresis, and the enzyme assay of the filtered amylase showed that the activity remained unchanged.**

***Index Terms*—Biomolecules, chemical vapor deposition, rapid thermal annealing, silicon nanoporous membrane.**

I. Introduction

THE separation of biomolecules based on their size and charge is one of the common practices in the field of biomolecular analysis for industrial and biomedical applications. Porous polymeric membranes are currently being used for this purpose [1]–[4], but they have the disadvantage that the molecules take a long time to pass through the porous structure and the molecules can get stuck in the meandering pores. Silicon nanoporous membranes (SNMs), which can be made as thin as the size of the molecules themselves, are an attractive alternative for such applications [5]–[11]. The advantages of membrane thickness being comparable with the size of the molecules are lower sample loss and higher functional efficiency, without the fear of clogging.

Manuscript received September 22, 2012; accepted April 23, 2013. Date of publication June 3, 2013; date of current version July 3, 2013. This work was supported in part by the Department of Electronics and Information Technology (DeitY), Government of India. The review of this paper was arranged by Associate Editor Prof. J. Li.

The authors are with the Department of Electrical Engineering and Centre for NEMS and Nanophotonics, Indian Institute of Technology Madras, Chennai 600036, India (e-mail: hvbachar@gmail.com; sudeshnaiitm@gmail.com; enakshi@ee.iitm.ac.in).

Color versions of one or more of the figures in this paper are available online at http://ieeexplore.ieee.org.

Digital Object Identifier 10.1109/TNANO.2013.2262100

Different fabrication techniques have been reported for fabricating the SNMs, using processes such as electrochemical etching [12]–[14], E-beam [15], and focused ion beam (FIB) drilling [11], [16]. Membranes fabricated using electrochemical etching are several microns thick and they are often not suitable for biomolecular filtration because of their long and coarse-walled pores. FIB and E-beam techniques are sequential, and are not suitable for batch processing. As an alternative, Striemer *et al.* [17] reported that when a thin layer of amorphous silicon (a-Si) sandwiched between two oxide layers is subjected to rapid thermal annealing (RTA) at high temperatures, spontaneous voids are formed in the material. Our strategy is to fabricate SNMs using this technique, but using plasma-enhanced chemical vapor deposition (PECVD) for depositing the membrane material instead of RF magnetron sputtering reported by the authors, since PECVD allows better control on deposition and nucleation. We had previously reported on the fabrication of SNMs by depositing the a-Si layer using low-pressure chemical vapor deposition [18]. However, this procedure had the inherent disadvantage of higher thermal budget as well as a break in vacuum between the a-Si and oxide layer depositions.

In industrial processes, when enzymes and proteins are subjected to extensive purification steps, they tend to lose their activity. The use of nanoscale filters for enriching or separating important enzymes and proteins of low hydrodynamic diameters (d_h) by ultrafiltration, with minimum damage to the enzyme activity, is desirable. α-Amylase ($d_h \sim 6.4$ nm), bovine serum albumin (BSA, $d_h \sim 8$ nm), catalase ($d_h \sim 9$ nm) and xanthine oxidase ($d_h \sim 13.6$ nm) are globular proteins with increasing hydrodynamic diameters [19]–[23]. The functional diameter of the pores in the SNMs is decided by the protein structure and the electrostatic interactions of the protein with the membrane material [17]. The surface charges of these proteins, obtained from the ASA-VIEW images [24] indicate that maximum number of negative surface charges are present in catalase (45 amino acids), followed by BSA (33 amino acids), xanthine oxidase (19 amino acids), and α-amylase (17 amino acids). A permeability study of these industrially important biomolecules with increasing d_h can be used to characterize the functional diameter of the pores.

In this study, the ultrathin SNMs were fabricated using microelectronics fabrication processes involving PECVD and RTA. The permeability of functionally important biomolecules with varying d_h and surface charge has been studied using the fabricated SNMs. The movement of biomolecules under simple diffusion in the presence of an electric field and the effect of

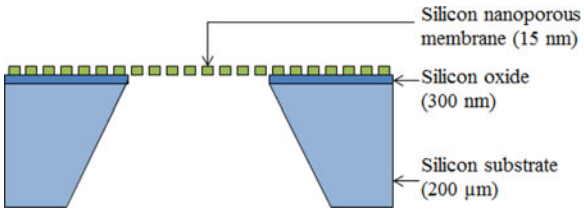

Fig. 1. Cross-sectional schematic of the SNM supported on silicon substrate.

varying the pH of the solution were analyzed to understand the role of the functional diameter of the nanopores in the permeability of the biomolecules through the SNMs. The physical integrity of the filtered proteins was studied and the functionality of amylases after filtration was tested.

II. Experiments

A. Fabrication of SNMs

The fabrication of SNMs has been described by us previously in [18]. Some changes have been incorporated in the present process steps. A thin layer of a-Si of 15 nm thickness, sandwiched between two layers of silicon oxide (SiO_x) of 300 nm thickness was deposited on the unetched surface of the bare silicon wafer using PECVD (Oxford Plasma Technology, Oxford, UK). The oxide layers were deposited from silane and nitrous oxide chemistry at a temperature of 250 °C, chamber pressure of 200 mTorr, and RF power of 20 W. The a-Si layer was deposited from 10% silane diluted with hydrogen at the same temperature, pressure, and power mentioned earlier. The deposition recipes were previously standardized by us to deposit the layers with accurate thickness control and repeatability. The wafer was subjected to RTA (AnnealSys, Montpellier, France) at a temperature of 850 °C and ramp rate of 50 °C/s, for 30 s in nitrogen ambient. During this process, the a-Si layer was transformed into nanocrystalline silicon (nc-Si) with voids in between the crystal structures. Voids were formed due to the nonavailability of sufficient Si atoms in the ultrathin layer and the vertical confinement between the two oxide layers [17]. The voids spanned the entire thickness of the nc-Si layer, thus forming through-nanopores. The diameter and density of the nanopores were found to be dependent on the annealing temperature. The release of the membrane was done by dry etching of the silicon followed by the stripping of the oxide layers sandwiching the membrane using buffered HF. Fig. 1 shows the schematic of the cross section of a typical SNM.

B. TEM Imaging

Plan-view high-resolution transmission electron microscopy (TEM) images of SNMs were obtained to determine the size and density of pores in the membrane. The silicon samples were diced into pieces of dimensions 3 mm × 6 mm with the membrane at the center, as required by the specimen holder of the TEM equipment (CM120, Philips). Each membrane was imaged at several places in order to get an overall picture of the pore size distribution and pore density. Images of several membranes fabricated similarly were obtained to study the repeatability of the process. The diameters of the pores were determined from the TEM images using the freeware image processing tool called ImageJ [25].

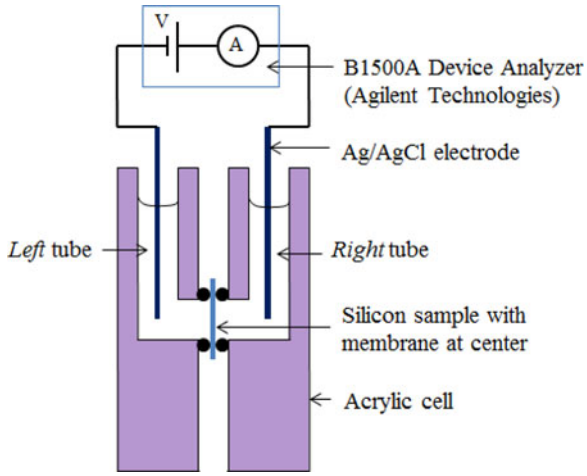

Fig. 2. Schematic diagram of the setup used for ionic conduction and diffusion experiments. The electrodes were absent during the diffusion experiments.

C. Ionic Conduction Through Nanopores

In order to confirm the presence of through-nanopores in the membranes, ionic conduction through the SNMs was measured using a custom-made acrylic setup (see Fig. 2). The setup has two reservoirs named left and right for convenience, separated by the silicon chip of size 14 mm × 14 mm containing one SNM of size approximately 220 μm × 220 μm at the center. The connection between the two reservoirs was possible only through the nanopores, as it was perfectly sealed with two silicone O-rings. After mounting the chip onto the setup, the two reservoirs were filled with the potassium chloride (KCl) solution of known concentration and pH, and set aside for 4 h to hydrate the nanopores. Two Ag/AgCl electrodes were immersed, one in each reservoir, to apply the voltage across the membrane and to measure the resulting ionic current. The current voltage ($I - V$) characteristics of the SNMs were obtained by sweeping the voltage (B1500 A, Agilent Technologies, CA, USA) from –1 to +1 V in steps of 100 mV. The KCl concentration was varied over five orders of magnitude from 0.1 mM to 1 M in the ascending order, and for each concentration, the $I - V$ characteristics were obtained with the same membrane. The entire experiment was repeated with several SNMs fabricated similarly for repeatability study.

D. Permeability Study of Biomolecules Through Nanoporous Membranes

The permeability of biomolecules through SNMs was studied using α-amylase (Fluka, Germany), BSA (SRL, India), catalase, and xanthine oxidase (Sigma-Aldrich, India) molecules. 300 μl of 0.1 M phosphate buffer solution (PBS) at pH 7.0 was added simultaneously to the left and right tubes of the acrylic setup (see Fig. 2, without electrodes) and was kept aside for 4 h to hydrate the nanopores. The PBS was then pipetted out from both the tubes and 300 μl of biomolecular solution prepared

at a concentration of 0.2 mg/ml was loaded in the left tube. Simultaneously, 300 μl of PBS buffer was loaded in the right tube in order to avoid any pressure imbalance on the membrane. After 10 min, 200 μl of liquid from each tube was assayed using the bicinchoninic acid (BCA) method as per its standard protocol [22]. The absorbance (optical density or O.D.) of assays was measured at the wavelength of 562 nm which gave the concentration of the molecules in each tube. The BCA method can detect protein concentrations over the range 0.5–1500 μg/ml. The entire process was repeated for diffusion times of 20, 30, and 60 min with the same membrane.

Diffusion of biomolecules through the nanopores is dependent not just on the size of the molecules, but also on the electrostatic interactions of the molecules with the pore walls. Biomolecules and silicon surfaces are known to possess surface charges when in contact with liquid media [26]. In particular, the surface charges change with the pH of the solution in which the molecules are suspended. At a particular pH, which is the characteristic of the molecule, the surface bears no net charge, and this pH is called the isoelectric pH (IEP) of the molecule [27]. If the pH of the solution is greater than IEP, then the molecule surface bears net negative charge, and if the pH is lesser than IEP, then it bears net positive charge. In order to obtain an insight into the permeability of the SNMs for differently charged molecules, the pH of the buffer was changed, which in turn changed the polarity of the surface charges on the molecules. Two pH values of 7 and 3 were chosen for this study, and the diffusion experiments were conducted for 1 h each, with α-amylase (IEP $= 5.4$) and BSA (IEP $= 4.7$) molecules. At pH 7, both the molecules had negative surface charges, while at pH 3, both have positive surface charges. The pore walls and the membrane surface, which had hydroxyl groups at the interface with the solution due to the native oxide formation, have negative surface charges at both these pH values [28].

E. Verification Tests for the Physical Integrity and Functionality of the Filtered Proteins

The filtered α-amylase and BSA molecules were tested by the sodium dodecyl sulfate polyacrylamide gel electrophoresis (SDS-PAGE) method [29]. The protein molecules bound to SDS become linearized and move in the gel toward the anode on the basis of their molecular weights only. Hence, any cleavage in the protein molecule will lead to multiple bands in SDS-PAGE. α-Amylase and BSA samples from both the left and right tubes were heated with SDS at 95 °C for 10 min and loaded on a 12% SDS-PAGE.

α-Amylase activity was analyzed from the samples collected from both the left and right tubes by the method of Bernfeld [30]. The amount of reducing sugar released was quantified using 3,5-dinitrosalicylic acid (DNS) reagent with maltose as standard. 1 ml of reaction mixture consisting of 500 μl of 1% soluble starch (prepared in 100 mM sodium phosphate buffer, pH 7.5), 475 μl of the enzyme buffer (0.1 M PBS), and 25 μl of enzyme samples from both the left and right tubes were incubated for 15 min at 55 °C. An enzyme blank with DNS added before the addition of enzyme at 55 °C was used as control. The reactions were stopped by heat inactivation, and the maltose released from starch by the amylase activity in the enzyme mixes was assayed. One unit of enzyme releases from soluble starch, one micromole of reducing groups (calculated as maltose) per minute at 25 °C and pH 6.9 under the specified conditions. 3 ml of reaction mixture contained DI water, maltose (released from starch in above described amylase reactions), and DNS reagent. Different concentrations of maltose when reacted with DNS reagent developed different gradations of color which was measured by noting the change in the O.D. at 540 nm.

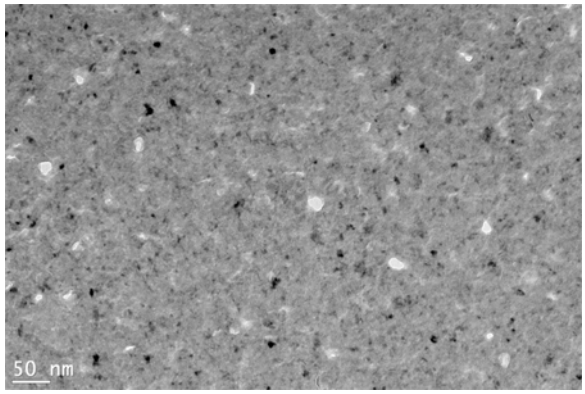

Fig. 3. Plan-view TEM image of the SNM which was subjected to RTA at 850 °C. The white spots are nanopores, the gray areas are amorphous regions, and the black spots are the crystalline nucleation centers.

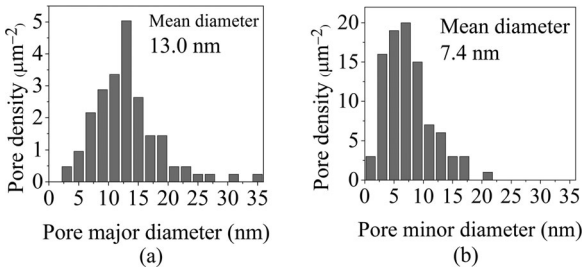

Fig. 4. Distributions of (a) major and (b) minor diameter values of the pores in the SNM.

III. Results and Discussions

A. TEM Imaging

Fig. 3 shows the TEM image of the SNM which was annealed at 850 °C. The white spots in the image are nanopores, the gray areas are amorphous regions, and the black spots are crystalline regions of the membrane. Since the shape of the pores was elliptical and sometimes irregular, two diameter values were computed for each pore—the major diameter, which was the longest diameter of the pore, and the minor diameter, which was the shorter diameter at the perpendicular direction to the major axis. Fig. 4 shows the histograms depicting the distributions of the major and minor diameters of the pores in the SNM. The major diameter values varied between 3 and 35 nm with an average value of 13 nm, whereas the minor diameter values ranged from 1 to 21 nm with an average of 7.4 nm. The density of the pores peaked at the average value, with densities falling

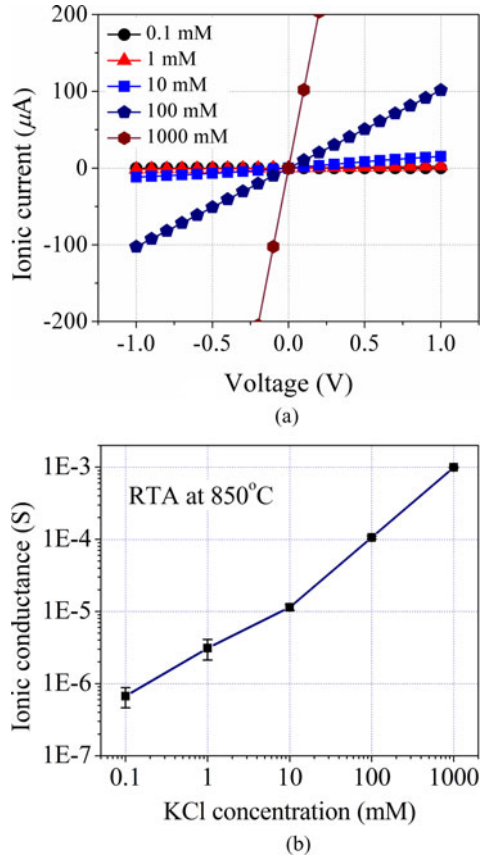

Fig. 5. (a) $I - V$ characteristics of the SNM with electrolytes of different concentrations. (b) Ionic conductance of SNMs versus concentration of electrolyte.

on either sides of the peak. The difference in the distributions of major and minor diameter values shows that the majority of the pores were elliptical in shape. However, this is not a serious drawback for filtration of biomolecules through the pores. The biomolecules used in this work were all globular, which assumed spheroidal shapes when dispersed in the buffer solution. The minor diameter values decide the cutoff size of molecules that can pass through the SNMs. The pore sizes and density were found to be dependent on annealing parameters, the detailed study of which is in progress.

B. Ionic Conduction

Fig. 5(a) shows the $I - V$ characteristics of the SNMs. The ionic current, which was due to the passage of K^+ and Cl^- ions across the membrane through the nanopores, showed linear variations with the voltage for concentrations between 1 and 1000 mM of KCl. A control sample with a membrane sans the nanopores showed currents in femtoamperes, regardless of the applied voltage and KCl concentration. This confirmed that the ionic conduction was indeed taking place through the nanopores and not through any imperfections (if any) in the setup. Different SNMs fabricated under the same conditions gave almost the same conductance for the given KCl concentration, as indicated by the error bars in the conductance versus the KCl concentration graph of Fig. 5(b), indicating that there was little variation

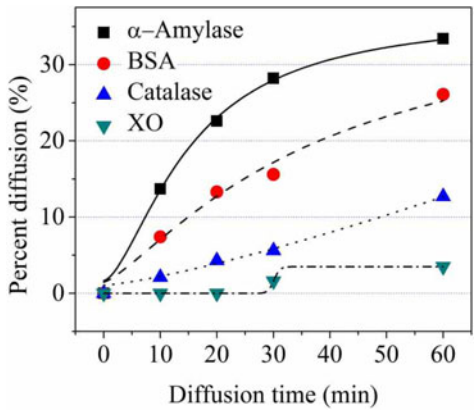

Fig. 6. Percentage diffusion of biomolecules through the SNM, with 0.1 M PBS at pH 7.0.

in the pore size and density from sample to sample. This makes the fabrication method suitable for batch processing.

C. Permeability of Biomolecules Through Nanoporous Membranes

Fig. 6 shows the results of diffusion of the biomolecules through the SNM. At all times, α-amylase ($d_h \sim 6.4$ nm) diffused more than the remaining molecules, whereas xanthine oxidase ($d_h \sim 13.6$ nm) was almost blocked by the membrane. This showed that even though the upper cutoff pore size as determined from the TEM images was much higher, the effective pore size was lesser. Electrical double layers at the pore walls [26] and electrostatic interactions between the molecules and pore walls are responsible for this difference. Among the remaining two molecules, even though BSA ($d_h \sim 8.0$ nm) and catalase ($d_h \sim 9.0$ nm) had comparable sizes, the percentage diffusion of BSA was greater than that of catalase. At pH 7, catalase possessing more negative charges than BSA [24] experienced greater electrostatic repulsion at the negatively charged pore walls. This is further borne out at pH 3 where both α-amylase and BSA molecules had net positive surface charges, and therefore got attached to the pore walls due to electrostatic attraction. The diffusion percentage of these molecules at pH 3 was very low at 3% even after 1 h of diffusion.

In this study, only globular proteins of known d_h have been considered. A preliminary permeability study with the total cell free extract from a filamentous fungus, *Eremothecium ashbyii*, containing proteins of various shapes and sizes demonstrated that some of the elongated proteins of higher molecular weights could also pass through these SNMs.

D. Structural and Functionality Test of the Filtered Proteins

The α-amylase and BSA samples from both the left and right tubes were run on a 12% SDS-PAGE to determine whether the two proteins were physically intact after diffusion across the SNMs. The presence of single bands at the same position in both the left and right samples for each protein indicated that the proteins were not cleaved after passing through the nanopores (see Fig. 7). Hence, it should be possible to filter

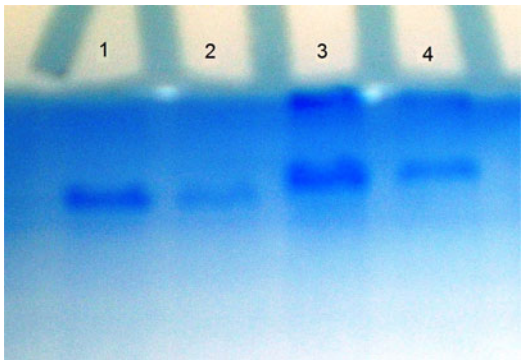

Fig. 7. Verification of the physical integrity of the proteins after diffusion through the nanoporous membranes. Lane 1: α-Amylase in left tube after 30 min. Lane 2: α-Amylase in right tube after 30 min. Lane 3: BSA in left tube after 30 min. Lane 4: BSA in right tube after 30 min.

biomolecules with $d_h \sim 8$ nm, such as enzymes, biomarkers, and those involved in drug delivery systems, microdialysis, etc., using these SNMs without any physical damage.

The α-amylase samples were also analyzed for enzyme activity by the method of Bernfeld [30]. The amount of reducing sugar released was quantified using DNS with maltose as standard. The experiments were done three times each and the average values were considered for calculating the specific activity. 290 μg maltose was produced by 0.186 μg amylase present in 25 μl of enzyme sample in the right tube. Similarly, 1061 μg maltose was produced by 0.668 μg α-amylase present in 25 μl of enzyme sample in the left tube. Thus the specific activity of α-amylase in the left and right tubes was the same and equal to 308 μmol/min per mg of the enzyme mix. This demonstrated that the specific activity of the enzyme was not altered after filtration indicating the possibility of using these SNMs for filtering or enriching industrially important enzymes of low hydrodynamic diameters without affecting their specific activities.

IV. Conclusion

SNMs of 15 nm thickness were fabricated by RTA of thin a-Si films deposited using PECVD. The SNMs were imaged using plan-view TEM which gave the distribution and density of pores in the samples. The presence of through-nanopores in the membranes was verified by measuring the ionic current through them for different concentrations of the electrolyte. Linear current voltage characteristics were measured, with the current in the range 2–850 μA, for KCl concentrations of 1–1000 mM, while the control sample with membrane but without nanopores showed currents in femtoampere regardless of the KCl concentration. The permeability of the SNMs to biomolecules of different hydrodynamic diameters was investigated by their diffusion studies. α-Amylase ($d_h \sim 6.4$ nm) could easily diffuse through the pores, whereas xanthine oxidase ($d_h \sim 13.6$ nm) was blocked. Diffusion rates of BSA ($d_h \sim 8$ nm) and catalase ($d_h \sim 9$ nm) were quite different, even though their sizes were comparable, due to the different surface charges that the molecules carry. The pH of the buffer played a significant role on the permeability. At pH 7, both α-amylase and BSA were negatively charged and diffused through the nanopores, whereas at pH 3, both were positively charged and did not diffuse, most probably due to attaching at the pore walls and membrane surface. The filtered proteins were found to remain physically uncleaved from SDS-PAGE data. The functionality of the filtered α-amylase was checked and found to be exactly the same as the unfiltered sample. Thus the batch processed SNMs can be used for diffusion controlled filtration systems and for isolating and enriching molecules from various microbial systems.

Acknowledgment

The authors would like to acknowledge Prof. T. S. Chandra, Department of Biotechnology, Indian Institute of Technology Madras for facilitating the bioassay work.

References

[1] M. Ulbricht, "Advanced functional polymer membranes," *Polymer*, vol. 47, pp. 2217–2262, 2006.
[2] S. Metz, C. Trautmann, A. Bertsch, and P. Renaud, "Polyimide microfluidic devices with integrated nanoporous filtration areas manufactured by micromachining and ion track etching," *J. Micromech. Mincroeng.*, vol. 14, pp. 324–331, 2004.
[3] L. T. Sexton, L. P. Horne, and C. R. Martin, "Developing synthetic conical nanopores for biosensing applications," *Mol. Biosyst.*, vol. 3, pp. 667–685, 2007.
[4] J. Han, J. Fu, and R. B. Schoch, "Molecular sieving using nanofilters: Past, present and future," *Lab Chip*, vol. 8, pp. 23–33, 2008.
[5] T. Tsuru, "Inorganic porous membranes for liquid phase separation," *Separation Purification Rev.*, vol. 30, no. 2, pp. 191–220, 2001.
[6] S. Kuiper, C. J. M. van Rijn, W. Nijdam, and M. C. Elwenspoek, "Development and applications of very high flux microfiltration membranes," *J. Membrane Sci.*, vol. 150, no. 1, pp. 1–8, 1998.
[7] T. A. Desai, T. West, M. Cohen, T. Boiarski, and A. Rampersaud, "Nanoporous microsystems for islet cell replacement," *Adv. Drug Del. Rev.*, vol. 56, pp. 1661–1673, 2004.
[8] A. M. Popa, P. Niedermann, H. Heinzelmann, J. A. Hubbell, and R. Pugin, "Fabrication of nanopore arrays and ultrathin silicon nitride membranes by block-copolymer-assisted lithography," *Nanotechnology*, vol. 20, p. 485303, 2009.
[9] R. Smith, "Biomedical applications employing microfabricated silicon nanoporous membranes," Ph.D. dissertation, Dept. of Elect. Eng. Comput. Sci., School of Graduate Studies, Case Western Reserve Univ., Cleveland, OH, USA, 2010.
[10] N. Ileri, P. Stroeve, A. Palazoglu, and J. W. Tringe, "Fabrication of functional silicon-based nanoporous membranes," *J. Micro/Nanolith. MEMS MOEMS*, vol. 11, no. 1, p. 013012, 2012.
[11] H. D. Tong, H. V. Jansen, V. J. Gadgil, and M. Elwenspoek, "Silicon nitride nanosieve membrane," *Nano Lett.*, vol. 4, pp. 283–287, 2004.
[12] A. A. Hamzah, J. Yunas, D. C. Fu, and B. Y. Majlis, "Electrochemically etched nanoporous silicon membrane for filtration of biological fluids," presented at the Int. Conf. Enabl. Sci. Nanotechnol., Kuala Lumpur, Malaysia, Dec. 1–3, 2010.
[13] M. Jaouadi, W. Dimassi, M. Gaidi, R. Chtourou, and H. Ezzaouia, "Nanoporous silicon membrane for fuel cells realized by electrochemical etching," *Appl. Surf. Sci.*, vol. 258, pp. 5654–5658, 2012.
[14] K. L. Chu, M. A. Shannon, and R. I. Masel, "Nanoporous silicon membrane based fuel cells for portable power sources applications," presented at the NanoScience and Technology Institute—Nanotechnology, Boston, FL, USA, 2006, vol. 1.
[15] M. J. Kim, M. Wanunu, D. C. Bell and A. Meller, "Rapid fabrication of uniformly sized nanopores and nanopore arrays for parallel DNA analysis," *Adv. Mater.*, vol. 18, pp. 3149–3153, 2006.
[16] Y. H. Lanyon, G. D. Marzi, Y. E. Watson, A. J. Quinn, J. P. Gleeson, G. Redmond, and D. W. M. Arrigan, "Fabrication of nanopore array electrodes by focused ion beam milling," *Anal. Chem.*, vol. 79, pp. 3048–3055, 2007.
[17] C. C. Striemer, T. R. Gaborski, J. L. McGrath, and P. M. Fauchet, "Charge and size based separation of macromolecules using ultrathin silicon membranes," *Nature Lett.*, vol. 445, pp. 749–753, 2007.

[18] H. V. B. Achar and E. Bhattacharya, "Nanoporous silicon membrane for biomolecular separation," *Int. J. Nanosci.*, vol. 10, pp. 793–796, 2011.
[19] M. B. Rao, A. M. Tanksale, M. S. Ghatge, and V. V. Deshpande, "Molecular and biotechnological aspects of microbial proteases," *Microbiol. Mol. Biol. Rev.*, vol. 62, pp. 597–635, 1998.
[20] S. Sivaramakrishnan, D. Gangadharan, K. M. Nampoothiri, and A. Pandey, "α-Amylases from microbial sources—An overview of recent developments," *Food Technol. Biotechnol.*, vol. 44, pp. 173–184, 2006.
[21] A. Aschi, N. Mbarek, M. Othman, and A. Gharbi, "Study of thermally and chemically unfolded conformations of bovine serum albumin by means of dynamic light scattering," *Mater. Sci. Eng. C*, vol. 28, pp. 594–600, 2008.
[22] P. K. Smith, R. I. Krohn, G. T. Hermanson, A. K. Mallia, F. H. Gartner, M. D. Provenzano, E. K. Fujimoto, N. M. Goeke, B. J. Olson, and D. C. Klenk, "Measurement of protein using bicinchoninic acid," *Anal. Biochem.*, vol. 150, pp. 76–85, 1985.
[23] J. Zhang, Q. Chi, B. Zhang, S. Dong, and E. Wang, "Molecular characterization of beef liver catalase by scanning tunneling microscopy," *Electroanalysis*, vol. 10, pp. 738–746, 1998.
[24] S. Ahmad, M. Gromiha, H. Fawareh, and A. Sarai, "ASAView: Database and tool for solvent accessibility representation in proteins," *BMC Bioinformat.*, vol. 5, no. 51, 2004.
[25] Image Processing and Analysis in JAVA. [Online]. Available: http://rsb.info.nih.gov/ij/
[26] R. B. Schoch, J. Han, and P. Renaud, "Transport phenomena in nanofluidics," *Rev. Modern Phys.*, vol. 80, pp. 839–883, 2008.
[27] M. Kosmulski, "The pH-dependent surface charging and the points of zero charge," *J. Colloid Interface Sci.*, vol. 253, pp. 77–87, 2002.
[28] S. Siddiqui, "Optimization of ammonia-peroxide water mixture for high volume manufacturing through surface chemical investigations," Ph.D. dissertation, Dept. of Material Science and Eng., Graduate College, Univ. Arizona, Tucson, AZ, USA, 2011.
[29] U. K. Laemmli, "Cleavage of structural proteins during the assembly of the head of bacteriophage T4," *Nature*, vol. 227, pp. 680–685, 1970.
[30] P. Bernfeld, "Amylases α and β," *Methods Enzymol*, vol. 1, pp. 149–158, 1955.

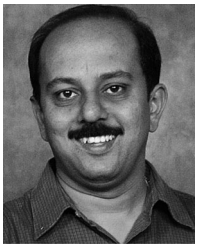

Balachandra H. V. Achar received the B.E. degree in electronics and communication engineering from the National Institute of Engineering, Mysore, India, and the M.Tech. degree in digital electronics from Manipal University, Manipal, India. He is currently working toward the Ph.D. degree from the Department of Electrical Engineering, Indian Institute of Technology Madras, Chennai, India.

Since 1999, he has been with the Manipal Institute of Technology, Manipal, where he is currently a senior-grade Assistant Professor. His research interests include microelectronics, MEMS, biosensors, and biomedical signal processing.

Sudeshna Sengupta received the M.Sc. degree in biophysics and molecular biology from Calcutta University, Kolkata, India, in 1997, and the Ph.D. degree from the Department of Biotechnology, Indian Institute of Technology (IIT) Madras, Chennai, India, in 2010.

She had been an Indo-Swiss Joint Research Program (ISJRP) Fellow and is currently engaged with her postdoctoral research on characterization and industrial application of nanoporous silicon membranes at the Centre for Nano Electromechanical systems (NEMS) and Nanophotonics, IIT Madras.

Enakshi Bhattacharya (M'10) received the M.Sc. degree in physics from Indian Institute of Technology (IIT) Bombay, Mumbai, India, in 1980, and the Ph.D. degree from TIFR Mumbai, Mumbai, in 1985.

She was a Postdoctoral Fellow at the National Renewable Energy Laboratory (then SERI), Golden, CO, USA, from 1986 to 1988. She was a faculty member in the Department of Physics, IIT Kanpur, from 1988 to 1991. Since 1991, she has been a faculty member of the Department of Electrical Engineering at IIT Madras, Chennai, India, where she is currently a Professor. She was a Visiting Scientist at the Micromachined Products Division of Analog Devices, USA, from 1999 to 2000. She is interested in all forms of silicon: single crystal, poly, amorphous, and porous and her current research interests include biosensors and MEMS.